

No large earthquakes in fully exposed subducted seamount

G. Bonnet^{1*}, P. Agard¹, S. Angiboust², M. Fournier¹, and J. Omrani³¹Sorbonne Université, CNRS-INSU, Institut des Sciences de la Terre de Paris, ISTeP UMR 7193, CNRS F-75005 Paris, France²Institut de Physique du Globe de Paris, Sorbonne Paris Cité, Université Paris Diderot, CNRS, F-75005 Paris, France³Geological Survey of Iran, Tehran, Iran

ABSTRACT

Bathymetric highs on the ocean floor ultimately sink into highly seismic subduction zones, raising vigorous debates on their potential to trigger or arrest large earthquakes ($M_w > 7.5$). Many geophysical and seismological studies addressing this problem meet penetration and/or resolution issues and deal with only the most recent earthquakes. We herein present the missing piece of the puzzle with the time-integrated field and petrographic record of a unique, almost intact subducted seamount cropping out along a fossil subduction interface. We document seamount buildup and subduction down to ~30 km, and we show that this seamount did not behave as a large earthquake asperity and may have acted as a barrier.

INTRODUCTION

The bathymetric roughness of seamounts and seamount chains entering subduction zones (Hillier and Watts, 2007; Bassett and Watts, 2015) has long been suspected to impact the geometry and seismic coupling of the subduction interface (Cloos and Shreve, 1996; Scholz and Small, 1997; Agard et al., 2018). Constraining the size and/or location of megathrust ruptures is critical for assessing earthquake hazard, and it is therefore of crucial importance to understand whether seamounts can limit large earthquake rupture propagation (acting as barriers) or may generate large earthquakes (acting as asperities; Cloos, 1992; Mochizuki et al., 2008; Wang and Bilek, 2011; Geersen et al., 2015; Saffer and Wallace, 2015). Despite spectacular geophysical imaging at the trench (Ranero and von Huene, 2000), seamounts are poorly imaged once subducted beyond ~15 km depth (Kodaira et al., 2000; Singh et al., 2011; Saffer and Wallace, 2015), and their internal deformation is thus beyond reach (Park et al., 1999). Fossil exhumed examples are scarce (MacPherson, 1983), yet they are of utmost interest because they possibly preserve millions of years of seamount evolution on the ocean floor and within the subduction zone.

AN EXCEPTIONALLY PRESERVED FOSSIL SEAMOUNT

Here, we report the discovery of a unique, fully exposed subducted seamount, namely, the Siah Kuh (SK) massif, and we present its

structure and evolution, which we detailed through extensive field and petrological data. This massif crops out within ophiolite fragments of the Neotethys Ocean subducted beneath Eurasia (Agard et al., 2011) in the easternmost portion of the Zagros Mountains, next to and below oceanic blueschists metamorphosed during the Late Cretaceous (Angiboust et al., 2016). This massif rises from Quaternary sediment infill as an 18 × 12-km-wide and ≥1.5-km-high feature (Figs. 1A and 1B), and it is composed of two subunits separated by tectonic contacts (Figs. 1C and 1D):

(1) An ~15 × 12 km oval-shaped unit (unit A) to the southwest is composed of up to 3 km of basaltic lava flows and pillow lavas intercalated with pillow breccia. Rhyodacitic subvolcanic rocks intruding this basaltic core are associated with lavas erupted on top of the basalts. Basalts and felsic lavas are overlain by a ≤500-m-thick Late Cretaceous sedimentary sequence, fully exposed on the southern flank of the unit. The base of this sequence consists of a massive limestone cap (10–50 m thick), of reef to lagoon affinity, with recrystallized fossil fragments like urchin spines, foraminifera, and gastropods. The top of the sequence is a variably thick (~100–500 m), mostly detrital, deepening-up sedimentary sequence of tuffaceous sandstone, red clay, pelagic limestone, and olistostromic debris flows. Pillow lavas (up to 1 km thick) emplaced conformably on top of these sediments indicate resumption of volcanic activity after sedimentation (Fig. 1).

(2) The smaller crescent-shaped unit to the northeast of SK (unit B) consists of, from bottom to top, serpentinites with meter- to decameter-large gabbroic pods and plagiogranites, a layer of massive gabbro overlain by rhyodacitic lavas, and finally kilometer-thick basaltic lavas without significant sedimentary cover.

While Unit B resembles classic ocean floor lithostratigraphy, the size and circular shape, amount of volcanism, shallow reef limestone cap—and overlying high-energy deposits (olistostromic sediments, debris flow)—indicate that unit A is a bathymetric anomaly on the seafloor, i.e., a seamount. The deepening-up sedimentary sequence hints at isostatic reequilibration of the oceanic lithosphere after the first magmatic event and/or seafloor subsidence.

Unit B was thrust southwestward onto unit A via a high-angle fault rooted in the lowermost, basal serpentinite horizon (Fig. 1D), suggesting initial strain localization beneath the oceanic Moho. Associated fault striations in gabbros strike N50° on average, parallel to the convergence direction during subduction beneath Eurasia (Agard et al., 2011). Smaller thrust faults of similar orientation rooted in sheared sediments (mainly tuffaceous sandstone and pelagic limestone) cut across the northeastern part of unit A and delineate tectonic subunits (A_{1-4} ; Fig. 1C). Small serpentinite bodies are pinched inside these faults, and basalts located in their vicinity lack significant deformation. The Oligocene Zagros collision (Agard et al., 2011) was responsible for the final arching of the whole SK massif into a south-to-southeast-vergent anticline (with locally tight refolded limbs; Fig. 1).

CONDITIONS OF BURIAL IN A SUBDUCTION ZONE

Former subduction of the SK seamount is indicated by a high-pressure–low-temperature (HP-LT) metamorphic imprint that postdates seafloor hydrothermal alteration and contact metamorphism near felsic intrusions. This tectonic

*E-mail: gbonnet01@gmail.com

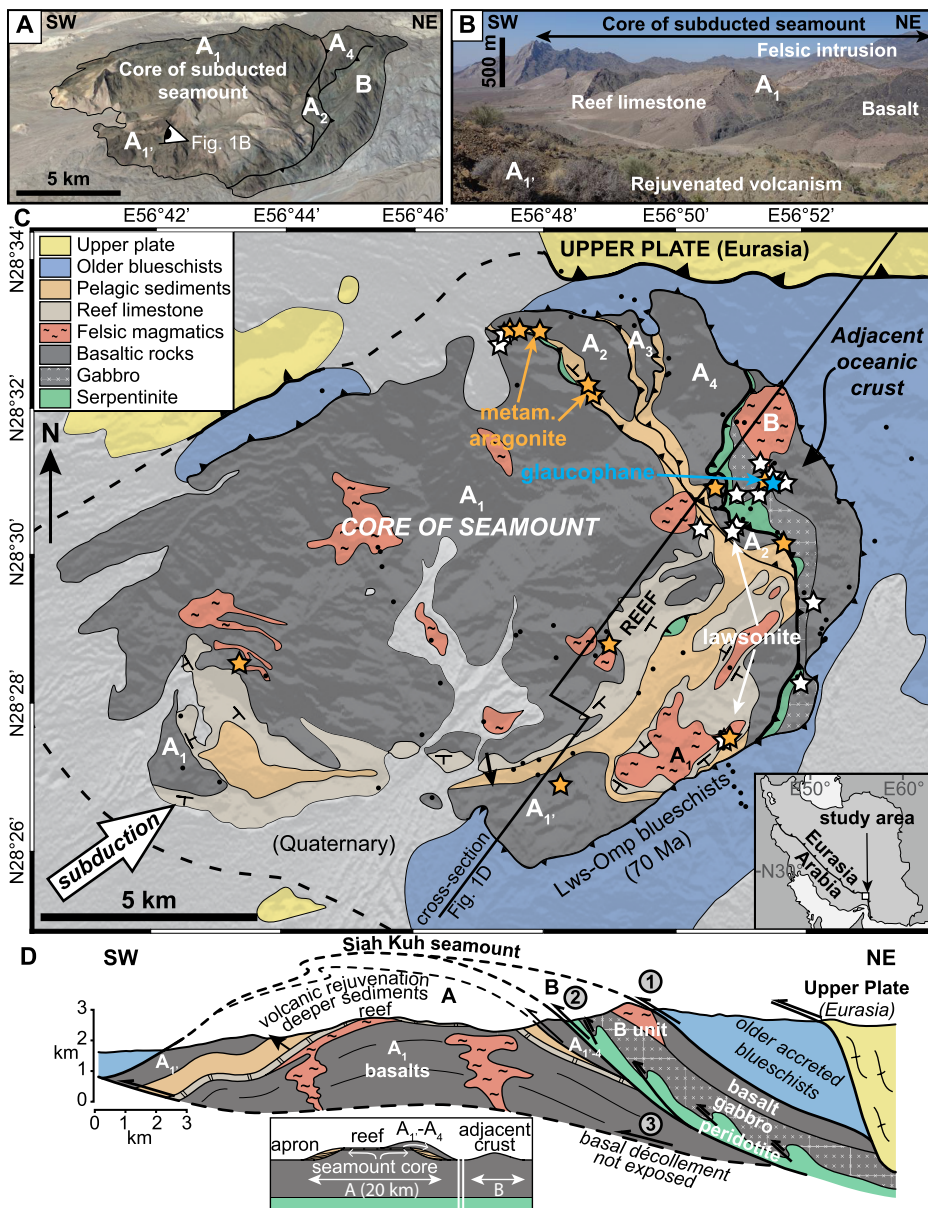


Figure 1. Geological overview of the Siah Kuh (SK) seamount. A: Satellite image of SK seamount showing different units. **B:** Photograph showing reef limestone capping basalts of seamount and later, rejuvenated volcanic activity. **C:** Geological map of SK seamount; black dots are sampling locations; inset is a large-scale map of Iran locating SK seamount. Lws-Omp—lawsonite-omphacite. **D:** Present-day section across SK seamount; successive locations of the plate interface (numbered 1–3) are highlighted; inset below: schematic restoration showing initial seamount architecture.

event is best expressed at the northeastern tip of the massif near the major shear zones bounding units A and B (Fig. 1). It consists of (1) sodium-bearing amphibole crystallization in gabbro, (2) numerous quartz-lawsonite veins in basalts, and (3) metamorphic aragonite veins in carbonates and basalts. These minerals are diagnostic of low-temperature subduction zone blueschists and define a minimum pressure of ~0.5 GPa, which, if lithostatic, corresponds to a minimum depth of ~20 km. The absence of jadeite + quartz in basalt, and the absence of antigorite + brucite in serpentinite argue for maximum pressures and temperatures of 0.9 GPa and 300 °C (~35 km).

Raman spectroscopy on organic matter-bearing metasediments from the middle part of the subducted seamount yielded an average temperature of 225 ± 30 °C (see the GSA Data Repository¹). Considering typical subduction gradients (<10 °C/km in mature subduction zones) and the ~7.5 °C/km inferred from lawsonite-omphacite blueschists formed early within the same

¹GSA Data Repository item 2019139, methods, detailed description of the pseudotachylyte, and Tables DR1 and DR2 (localization of metamorphic samples and representative chemical analyses), is available online at <http://www.geosociety.org/datarepository/2019/>, or on request from editing@geosociety.org.

subduction zone (Angiboust et al., 2016), pressures of 0.6–0.9 GPa are estimated at 225 °C. The paleosubduction depths of the SK seamount were thus around 25–35 km (Fig. 2A), i.e., within the seismogenic zone, where most large earthquakes occur (Oleskevich et al., 1999; Gao and Wang, 2014).

The original position of SK along the subduction zone is shown in Figure 3. The higher concentration of index HP-LT minerals in the northeastern part of SK (Fig. 1C) suggests greater burial depths, consistent with north-eastward subduction beneath Eurasia during Cretaceous and Paleocene times. Depth and temperature differences expected between the front and rear of an ~20-km-long seamount on a 20°-dipping slab are ~40 °C and 0.2 GPa, or 7 km depth. Importantly, only a minor part of the recorded 0.6–0.9 GPa may correspond to stress accumulation, which was estimated by numerical models with strain weakening (Ruh et al., 2017) to be ≤ 0.12 GPa ahead of a subducting seamount for almost dynamic fluid pressure ($\lambda = 0.9$). There is indeed strong argument that very high fluid pressures ($\lambda > 0.9$ –0.95) may prevail along the plate interface in the seismogenic zone (as can be inferred from the extremely low effective friction coefficients—typically 0.03; Gao and Wang, 2014), particularly in and at the front of subducting seamounts or ridges (Bell et al., 2010; Kato et al., 2010). Hydraulic brecciation, metamorphic vein formation (Fig. 2B), and chlorite-rich shear bands in metagabbro at peak pressure in SK further strengthen this conclusion. A minor contribution of tectonic overpressure-underpressure to pressure estimates would impact the inferred depth difference between the front and rear of the seamount, but it would not explain the HP-LT metamorphic record alone.

The SK seamount preserves pristine subduction-related deformation, as demonstrated by the spatial coincidence between faults and HP-LT metamorphism (Fig. 1C). Major displacements are localized in serpentinite (with an offset of several kilometers between units A and B; Fig. 1D) and in sediments (hectometer- to kilometer-scale offsets). Although the 25–35 km depth range is prone to brittle-ductile switches (Fagereng and den Hartog, 2017), the fact that deformation is mostly rooted in plastically deforming materials such as serpentinite and sediments suggests a dominantly ductile (creep) rather than brittle (potentially seismic) mechanical behavior. Long-term elevated pore-fluid pressure in these materials, as a result of metamorphic dehydration reactions and/or a sealed plate interface (Audet et al., 2009; Wallace et al., 2012; seamount-related—Bell et al., 2010) would favor ductile creep (as observed by Angiboust et al., 2016) and/or recurring brittle failure with earthquakes of only small magnitude.

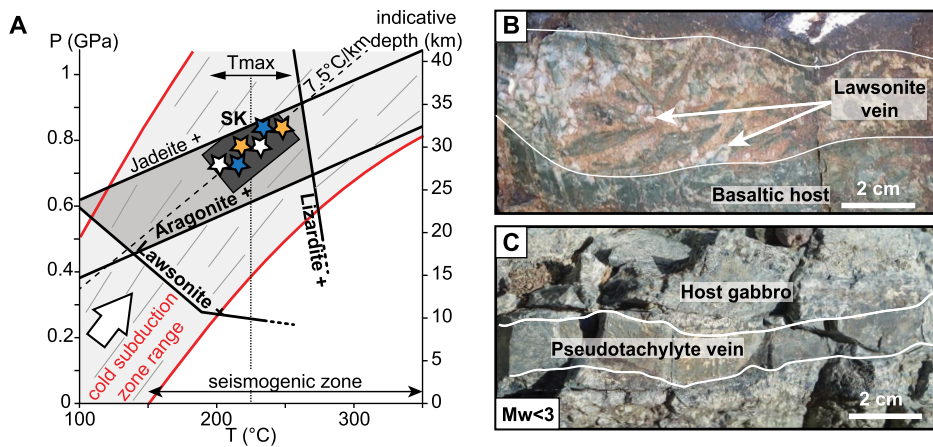


Figure 2. Subduction metamorphism and brittle deformation. A: Estimation of peak pressure-temperature (P - T) conditions reached by the Siah Kuh (SK) seamount during subduction, where stars for high-pressure metamorphism are only indicative of possible P - T conditions. B: Lawsonite vein in basalt testifying to hydraulic brecciation at high-pressure-low-temperature conditions. C: Pseudotachylyte vein in gabbro.

NO RECORD OF LARGE-MAGNITUDE EARTHQUAKES

Large-magnitude fossil earthquakes are commonly inferred from the presence of pseudotachylytes, i.e., glassy fault rocks formed by highly localized frictional heating during earthquakes (Austheim and Andersen, 2004; Di Toro et al., 2005) on large, kilometer-scale faults with significant amounts of slip (\geq meter scale). Extensive field investigations of the SK seamount revealed only one \sim 10-m-long pseudotachylyte (Fig. 2C) formed during subduction in gabbros of unit B (as shown by glaucophane crystallized from glass; see the

Data Repository), pointing to seismic events with maximum centimeter- to decimeter-scale slip (i.e., $M_w < \sim 2$ –3). This has important consequences for the seismic behavior of SK, as it shows that no major earthquake went through or was generated in the seamount during subduction. This demonstrates that the SK seamount did not host very large seismic rupture (Mochizuki et al., 2008; Wang and Bilek, 2011).

Whether the SK seamount behaved as a barrier is more difficult to assess, because megathrust earthquakes could tentatively have propagated outside the seamount without damaging it. Above the contact, however, no pseudotachylytes

or damage were observed in the upper plate (Fig. 1). The contact below, where slicing and detachment of the seamount from the subducting slab occurred prior to exhumation (Figs. 1D and 3), is unfortunately not exposed. With a plate convergence rate of ~ 5 cm/yr (Agard et al., 2011) and a 20-km-long seamount, detachment of the SK seamount must have lasted ~ 400 k.y. (only a fraction of a million years). This could in principle have been accommodated by creep or by ~ 2000 very large earthquakes if one $M_w \sim 8$ earthquake with ~ 1 –10 m slip occurred every 200 yr (as along Chile today). Yet, no major subduction earthquake affected SK, pointing again to deformation mostly by creep. We therefore propose (Fig. 3) that the SK seamount acted as a barrier to earthquake propagation on the subduction interface, possibly controlling the segmentation of seismic coupling (Geersen et al., 2015; Métois et al., 2016). Other examples of fossil and actively subducted seamounts should be sought to assess whether their size or structure may control their behavior as asperities and/or barriers.

The presence of sediments is commonly considered to smooth contact zones, to facilitate rupture propagation (Scholl et al., 2015; Shillington et al., 2015). In this exceptionally well-preserved seamount, the dearth of weak sediments, as, in fact, in most seamounts (Kodaira et al., 2000; Bassett and Watts, 2015), may have prevented the nucleation of large earthquakes. The presence of soft material (limited sediment intercalations—frequent in seamounts—and serpentinite) was nevertheless essential in promoting strain localization along the major contacts (Fig. 1C). The scarcity of exhumed seamounts in the geological record (MacPherson, 1983) indicates that effective decapitation of seamounts during subduction is generally impeded. We suggest that specific structural heterogeneities in the basal oceanic crust or within the seamount and/or strain localization into serpentinite (Ruh et al., 2015; Guillot et al., 2015), beneath the Moho (Fig. 3), are essential to prevent seamounts from sinking into the mantle.

ACKNOWLEDGMENTS

We thank E. Delairis (Institut des Sciences de la Terre de Paris [ISTeP]) for the preparation of thin sections, and O. Boudouma (ISTeP) and D. Deldicque (Ecole Normale Supérieure de Paris) for analytical support at the SEM. This study was funded by the project “Zooming in Between Plates” (Marie Curie International Training Network no. 604713).

REFERENCES CITED

- Agard, P., Omrani, J., Jolivet, L., Whitechurch, H., Vrielynck, B., Spakman, W., Monié, P., Meyer, B., and Wortel, M.J.R., 2011, Zagros orogeny: A subduction-dominated process: *Geological Magazine*, v. 148, p. 692–725, <https://doi.org/10.1017/S001675681100046X>.
- Agard, P., Plunder, A., Angiboust, S., Bonnet, G., and Ruh, J.B., 2018, The subduction plate interface: Rock record and mechanical coupling (from long

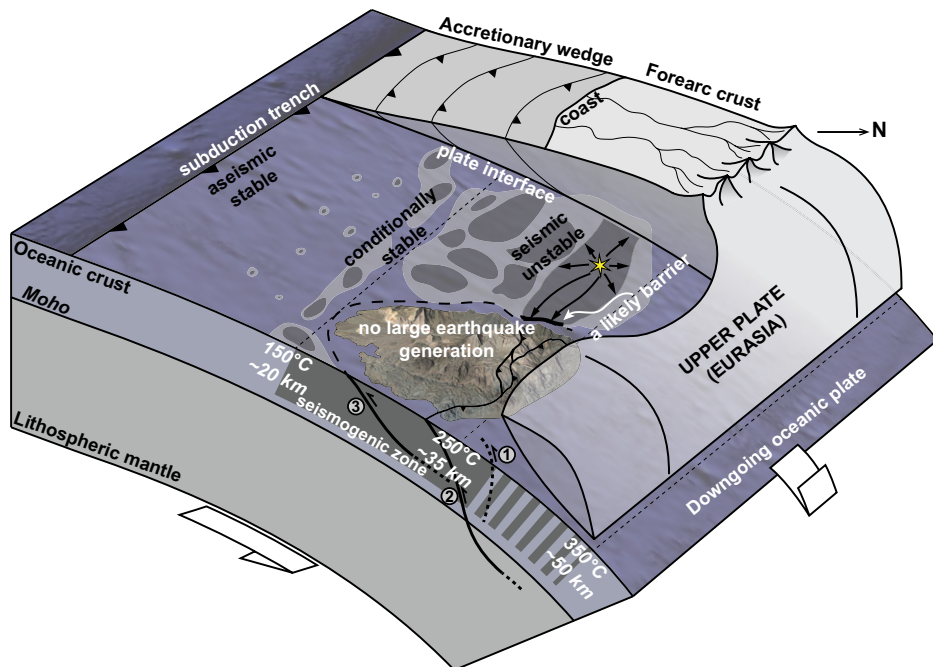


Figure 3. The Siah Kuh seamount shown in its former subduction environment within the seismogenic zone. Sketch suggests that the SK seamount did not generate large earthquakes, and that it likely acted as a barrier to propagation of earthquakes generated elsewhere on the subduction interface.

- to short timescales): *Lithos*, v. 320–321, p. 537–566, <https://doi.org/10.1016/j.lithos.2018.09.029>.
- Angiboust, S., Agard, P., Glodny, J., Omrani, J., and Oncken, O., 2016, Zagros blueschists: Episodic underplating and long-lived cooling of a subduction zone: *Earth and Planetary Science Letters*, v. 443, p. 48–58, <https://doi.org/10.1016/j.epsl.2016.03.017>.
- Audet, P., Bostock, M.G., Christensen, N.I., and Peacock, S.M., 2009, Seismic evidence for overpressured subducted oceanic crust and megathrust fault sealing: *Nature*, v. 457, p. 76–78, <https://doi.org/10.1038/nature07650>.
- Austrheim, H., and Andersen, T.B., 2004, Pseudotachylytes from Corsica: Fossil earthquakes from a subduction complex: *Terra Nova*, v. 16, p. 193–197, <https://doi.org/10.1111/j.1365-3121.2004.00551.x>.
- Bassett, D., and Watts, A.B., 2015, Gravity anomalies, crustal structure, and seismicity at subduction zones: 1. Seafloor roughness and subducting relief: *Geochemistry Geophysics Geosystems*, v. 16, p. 1508–1540, <https://doi.org/10.1002/2014GC005684>.
- Bell, R., Sutherland, R., Barker, D.H.N., Henrys, S., Bannister, S., Wallace, L.M., and Beavan, J., 2010, Seismic reflection character of the Hikurangi subduction interface, New Zealand, in the region of repeated Gisborne slow slip events: *Geophysical Journal International*, v. 180, p. 34–48, <https://doi.org/10.1111/j.1365-246X.2009.04401.x>.
- Cloos, M., 1992, Thrust-type subduction-zone earthquakes and seamount asperities: A physical model for seismic rupture: *Geology*, v. 20, p. 601–604, [https://doi.org/10.1130/0091-7613\(1992\)020<0601:TTSZEA>2.3.CO;2](https://doi.org/10.1130/0091-7613(1992)020<0601:TTSZEA>2.3.CO;2).
- Cloos, M., and Shreve, R.L., 1996, Shear zone thickness and the seismicity of Chilean- and Mariana-type subduction zones: *Geology*, v. 24, p. 107–110, [https://doi.org/10.1130/0091-7613\(1996\)024<0107:SZTATS>2.3.CO;2](https://doi.org/10.1130/0091-7613(1996)024<0107:SZTATS>2.3.CO;2).
- Di Toro, G., Nielsen, S., and Pennacchioni, G., 2005, Earthquake rupture dynamics frozen in exhumed ancient faults: *Nature*, v. 436, p. 1009–1012, <https://doi.org/10.1038/nature03910>.
- Fagereng, Å., and den Hartog, S.A.M., 2017, Subduction megathrust creep governed by pressure solution and frictional-viscous flow: *Nature Geoscience*, v. 10, p. 51–57, <https://doi.org/10.1038/ngeo2857>.
- Gao, X., and Wang, K., 2014, Strength of stick-slip and creeping subduction megathrusts from heat flow observations: *Science*, v. 345, p. 1038–1041, <https://doi.org/10.1126/science.1255487>.
- Geersen, J., Ranero, C.R., Barckhausen, U., and Reichert, C., 2015, Subducting seamounts control interplate coupling and seismic rupture in the 2014 Iquique earthquake area: *Nature Communications*, v. 6, p. 8267–8267, <https://doi.org/10.1038/ncomms9267>.
- Guillot, S., Schwartz, S., Reynard, B., Agard, P., and Prigent, C., 2015, Tectonic significance of serpentinites: *Tectonophysics*, v. 646, p. 1–19, <https://doi.org/10.1016/j.tecto.2015.01.020>.
- Hillier, J.K., and Watts, A.B., 2007, Global distribution of seamounts from ship-track bathymetry data: *Geophysical Research Letters*, v. 34, L13304, <https://doi.org/10.1029/2007GL029874>.
- Kato, A., et al., 2010, Variations of fluid pressure within the subducting oceanic crust and slow earthquakes: *Geophysical Research Letters*, v. 37, <https://doi.org/10.1029/2010GL043723>.
- Kodaira, S., Takahashi, N., Nakanishi, A., Miura, S., and Kaneda, Y., 2000, Subducted seamount imaged in the rupture zone of the 1946 Nankaido earthquake: *Science*, v. 289, p. 104–106, <https://doi.org/10.1126/science.289.5476.104>.
- MacPherson, G.T., 1983, The Snow Mountain volcanic complex: An on-land seamount in the Franciscan terrain, California: *The Journal of Geology*, v. 91, p. 73–92, <https://doi.org/10.1086/628745>.
- Métóis, M., Vigny, C., and Socquet, A., 2016, Interseismic coupling, megathrust earthquakes and seismic swarms along the Chilean subduction zone (38°–18°S): *Pure and Applied Geophysics*, v. 173, p. 1431–1449, <https://doi.org/10.1007/s00024-016-1280-5>.
- Mochizuki, K., Yamada, T., Shinohara, M., Yamanaka, Y., and Kanazawa, T., 2008, Weak interplate coupling by seamounts and repeating M~7 earthquakes: *Science*, v. 321, p. 1194–1197, <https://doi.org/10.1126/science.1160250>.
- Oleskevich, D.A., Hyndman, R.D., and Wang, K., 1999, The updip and downdip limits to great subduction earthquakes: Thermal and structural models of Cascadia, south Alaska, SW Japan, and Chile: *Journal of Geophysical Research—Solid Earth*, v. 104, p. 14,965–14,991, <https://doi.org/10.1029/1999JB900060>.
- Park, J.O., Tsuru, T., Kaneda, Y., Kono, Y., Kodaira, S., Takahashi, N., and Kinoshita, H., 1999, A subducting seamount beneath the Nankai accretionary prism off Shikoku, southwestern Japan: *Geophysical Research Letters*, v. 26, p. 931–934, <https://doi.org/10.1029/1999GL900134>.
- Ranero, C.R., and von Huene, R., 2000, Subduction erosion along the Middle America convergent margin: *Nature*, v. 404, p. 748–752, <https://doi.org/10.1038/35008046>.
- Ruh, J.B., Le Pourhiet, L., Agard, P., Burov, E., and Gerya, T.V., 2015, Tectonic slicing of subducting oceanic crust along plate interfaces: Numerical modeling: *Geochemistry Geophysics Geosystems*, v. 16, p. 3505–3531, <https://doi.org/10.1002/2015GC005998>.
- Ruh, J.B., Sallarès, V., Ranero, C.R., and Gerya, T.V., 2017, Crustal deformation dynamics and stress evolution during seamount subduction: High-resolution 3-D numerical modeling: *Journal of Geophysical Research—Solid Earth*, v. 121, p. 6880–6902, <https://doi.org/10.1002/2016JB013250>.
- Saffer, D.M., and Wallace, L.M., 2015, The frictional, hydrologic, metamorphic and thermal habitat of shallow slow earthquakes: *Nature Geoscience*, v. 8, p. 594–600, <https://doi.org/10.1038/ngeo2490>.
- Scholl, D.W., Kirby, S.H., von Huene, R., Ryan, H., Wells, R.E., and Geist, E.L., 2015, Great ($\geq M_w$ 8.0) megathrust earthquakes and the subduction of excess sediment and bathymetrically smooth seafloor: *Geosphere*, v. 11, p. 236–265, <https://doi.org/10.1130/GES01079.1>.
- Scholz, C.H., and Small, C., 1997, The effect of seamount subduction on seismic coupling: *Geology*, v. 25, p. 487–490, [https://doi.org/10.1130/0091-7613\(1997\)025<0487](https://doi.org/10.1130/0091-7613(1997)025<0487).
- Shillington, D.J., Bécel, A., Nedimović, M.R., Kuehn, H., Webb, S.C., Abers, G.A., Keranen, K.M., Li, J., Delescluse, M., and Mattei-Salicrup, G.A., 2015, Link between plate fabric, hydration and subduction zone seismicity in Alaska: *Nature Geoscience*, v. 8, p. 961–964, <https://doi.org/10.1038/ngeo2586>.
- Singh, S.C., et al., 2011, Aseismic zone and earthquake segmentation associated with a deep subducted seamount in Sumatra: *Nature Geoscience*, v. 4, p. 308–311, <https://doi.org/10.1038/ngeo1119>.
- Wallace, L.M., Fagereng, A., and Ellis, S., 2012, Upper plate tectonic stress state may influence interseismic coupling on subduction megathrusts: *Geology*, v. 40, p. 895–898, <https://doi.org/10.1130/G33373.1>.
- Wang, K., and Bilek, S.L., 2011, Do subducting seamounts generate or stop large earthquakes?: *Geology*, v. 39, p. 819–822, <https://doi.org/10.1130/G31856.1>.

Printed in USA